Thermochemistry of $La_{1-x}Sr_xFeO_{3-\delta}$ Solid Solutions ($0.0 \leq x \leq 1.0$, $0.0 \leq \delta \leq 0.5$)

Jihong Cheng and Alexandra Navrotsky*

Thermochemistry Facility and NEAT ORU, University of California at Davis, One Shields Avenue, Davis, California 95616

Xiao-Dong Zhou and Harlan U. Anderson

Electronic Materials Applied Research Center, University of Missouri−Rolla, Rolla, Missouri 65401

Received August 18, 2004. Revised Manuscript Received February 17, 2005

A series of compounds with the general formula $La_{1-x}Sr_xFeO_{3-\delta}$ have been synthesized in the complete solid solution range $0.0 \leq x \leq 1.0$ and $0.0 \leq \delta \leq 0.5$ with a variety of heat treatments. High-temperature drop solution calorimetry in molten $2PbO{\cdot}B_2O_3$ at 702 °C was performed to determine their enthalpies of formation from oxides at room temperature. The enthalpy of oxidation involved in the reaction $2Fe^{\times}_{Fe} + V^{\bullet\bullet}_{O} + 0.5O_2(g) = 2Fe^{\bullet}_{Fe} + O^{\times}_{O}$ is independent of oxygen nonstoichiometry in each $La_{1-x}Sr_xFeO_{3-\delta}$ series with a given x, and further is approximately constant at -200 ± 50 kJ/mol O_2 for $0 < x \leq 0.5$ and -140 ± 30 kJ/mol O_2 for $0.5 < x < 1.0$. The enthalpies of formation from oxides in the $LaFeO_3$−$SrFeO_{2.5}$ solid solution can be fitted either by a quadratic equation or by two straight line segments intersecting at $x = 0.5$. The quadratic fit gives a positive interaction parameter, 36.1 ± 4.9 kJ/mol, suggesting a tendency toward phase separation. The two linear segment models two regions of oxygen vacancy presence: dilute (random distribution) for $x \leq 0.5$ and concentrated (short-range ordering) for $x > 0.5$. Extrapolation to the end-member ($x = 1$) gives the enthalpy of formation of perovskite-type $SrFeO_{2.5}$ and the enthalpy of the hypothetical brownmillerite−perovskite phase transition at room temperature is estimated as 5.5 ± 4.0 kJ/mol. This small value implies extensive short-range order in the perovskite phases with high x. The enthalpies of formation from oxides in the $LaFeO_3$−$SrFeO_3$ solid solution are virtually independent of Sr composition when $x \leq 0.67$ and are a few kJ/mol more exothermic when $x \geq 0.7$. This is interpreted by phase evolutions from low symmetries to cubic.

1. Introduction

Solid oxide fuel cells (SOFCs) are promising power generation devices for more efficient and cleaner energy.[1] A single cell basically consists of a dense, oxygen ion conducting solid electrolyte sandwiched between two porous electrodes (the anode and cathode). Conventional cathodes use Sr-doped $LaMnO_3$ perovskites (LSM) that only conduct electronically.[2] Oxygen molecules are ionized solely at the triple-phase boundary (TPB) where oxygen gas, cathode, and electrolyte meet. A good cathode material needs to be an excellent mixed ionic and electronic conductor (MIEC), so the reaction zone is able to extend from the TPB over the entire cathode surface.

A number of other alkaline earth-doped perovskites (ABO_3, A = La, B = first-row transition metals) have been proposed as good MIECs.[3−7] Sr-doped $LaCoO_3$ perovskites (LSC) exhibit substantial ionic and electronic conductivity[8] and show superior oxygen exchange and bulk diffusion characteristics to LSM,[9] but their thermal expansion coefficient (TEC) is exceptionally high,[10] which causes thermal expansion mismatch between the electrode and the electrolyte during repeated thermal cycling. In contrast, Sr-doped $LaFeO_3$ perovskites (LSF) have a better-matched TEC while maintaining high mixed conductivity and good catalytic activity for oxygen reduction.[7] In addition, LSF tends to react more slowly with the yttria-stabilized zirconia (YSZ) electrolyte than LSM and LSC at the SOFC operating temperature (∼1000 °C).[11,12]

The unique electrical properties of $La_{1-x}Sr_xFeO_{3-\delta}$ perovskites are closely related to the defect chemistry

* To whom correspondence should be addressed. Tel.: (530)752-3292. Fax: (530)752-9307. E-mail: anavrotsky@ucdavis.edu.

(1) Minh, N. Q. *J. Am. Ceram. Soc.* **1993**, *76*, 563.
(2) Hammouche, A.; Schouler, E. L.; Henault, M. *Solid State Ionics* **1988**, *28−30*, 1205.
(3) Kuscer, D.; Hanzel, D.; Holc, J.; Hrovat, M.; Kolar, D. *J. Am. Ceram. Soc.* **2001**, *84*, 1148.
(4) Petrov, N.; Kononchuk, O. F.; Andreev, A. V.; Cherpanov, V. A.; Kofstad, P. *Solid State Ionics* **1995**, *80*, 189.
(5) Nagamoto, H.; Mochida, I.; Kagotani, K.; Inoue, H. *J. Mater. Res.* **1993**, *8*, 3158.
(6) Mantzavinos, D.; Hartley, A.; Metcalfe, I. S.; Sahibzada, M. *Solid State Ionics* **2000**, *134*, 103.
(7) Huang, K.; Lee, H. Y.; Goodenough, J. B. *J. Electrochem. Soc.* **1998**, *145*, 3220.
(8) Mizusaki, J.; Tabuchi, J.; Matsuura, T.; Yamauchi, S.; Fueki, K. *J. Electrochem. Soc.* **1989**, *136*, 2082.
(9) ten Elshof, J. E.; Lankorst, M. H. R.; Bouwmeester, H. J. M. *Solid State Ionics* **1997**, *99*, 15.
(10) Ohno, Y.; Nagata, S.; Sato, H. *Solid State Ionics* **1983**, *9/10*, 1001.
(11) Yokokawa, H.; Sakai, N.; Kawada, T.; Dokiya, M. In *Proceedings of the International Symposium on Solid Oxide Fuel Cells*; Yamamoto, O., Dokiya, M., Tagawa, H., Eds.; Science House: Tokyo, Japan, 1990; pp 118−134.
(12) Yokokawa, H.; Sakai, N.; Kawada, T.; Dokiya, M. *Solid State Ionics* **1992**, *52*, 43.

10.1021/cm048613o CCC: $30.25
Published on Web 03/23/2005

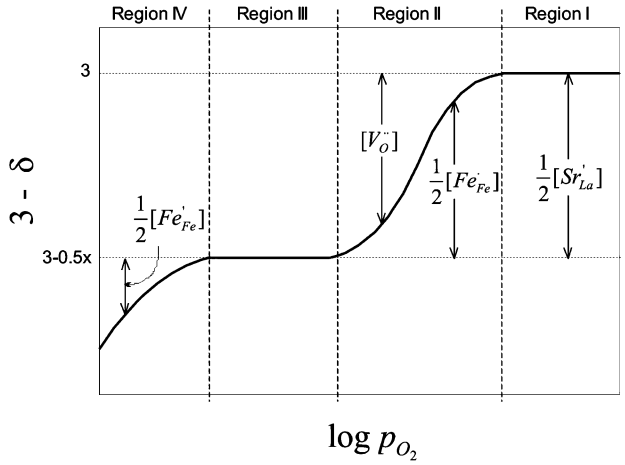

Figure 1. A schematic representation of the concentrations of defects in a $La_{1-x}Sr_xFeO_{3-\delta}$ sample as a function of oxygen partial pressure at a given temperature.[14]

involved. Upon the substitution of strontium for lanthanum, the difference in ionic charge between Sr^{2+} and La^{3+} must be compensated. Oxidation of other species in the structure, such as (formally) Fe^{3+} to Fe^{4+}, or a creation of oxygen vacancies ($\delta > 0$) can balance the charge. Mizusaki et al.[13,14] proposed a point defect model, in which the major defects in $La_{1-x}Sr_xFeO_{3-\delta}$ are Sr'_{La}, $V_O^{\bullet\bullet}$, $Fe^{\bullet}_{Fe}(Fe^{4+})$, and $Fe'_{Fe}(Fe^{2+})$, where Kröger−Vink notation[15] is taken. For a given Sr composition, the defect concentrations are functions of the oxygen partial pressure (p_{O_2}) and the temperature (T). A schematic diagram of the defect concentrations as a function of p_{O_2} for a $La_{1-x}Sr_xFeO_{3-\delta}$ sample is given in Figure 1.

Under strongly oxidizing atmospheres (Region I in Figure 1), oxygen nonstoichiometry is negligible ($\delta \approx 0$). The defect equation can be represented by

$$Fe^{\times}_{Fe} + Sr^{\times}_{Sr} = Sr'_{La} + Fe^{\bullet}_{Fe} \qquad (1)$$

With decreasing p_{O_2}, oxygen vacancies are formed at the cost of Fe^{4+} and $V_O^{\bullet\bullet}$ coexists with $Fe^{\bullet}_{Fe}$ (Region II):

$$2Fe^{\bullet}_{Fe} + O^{\times}_{O} = 2Fe^{\times}_{Fe} + V_O^{\bullet\bullet} + 0.5O_2(g) \qquad (2)$$

While p_{O_2} is reduced further (Region III), the concentration of $Fe^{\bullet}_{Fe}$ becomes sufficiently low and the plateau corresponds to $\delta \approx 0.5x$. In very reducing atmospheres (Region IV), some Fe^{3+} ions are reduced to Fe^{2+} while generating more oxygen vacancies:

$$2Fe^{\times}_{Fe} + O^{\times}_{O} = 2Fe'_{Fe} + V_O^{\bullet\bullet} + 0.5O_2 \qquad (3)$$

We note that eqs 1−3 denote formal oxidation states of Fe and make no assumptions about the delocalization of holes or electrons. The electronic conduction in $La_{1-x}Sr_xFeO_{3-\delta}$ is usually attributed to the hopping of electron holes between Fe ions with different valence states and the ionic conduction comes from the migration of oxygen vacancies in the oxygen sublattice.

Practically, thermodynamic data are of critical importance to evaluate and predict the stability and compatibility of components at fuel cell operating temperatures. From the fundamental point of view, the solid solution in $La_{1-x}Sr_xFeO_{3-\delta}$ is completely miscible and thus provides a unique opportunity for studying the thermodynamic behavior of complex oxides with rich defect chemistry. Unfortunately, studies in the literature are rather limited. Mizusaki and coworkers[14,16] determined with thermogravimetry the enthalpy and entropy of oxidation as functions of oxygen partial pressure and temperature for $0.0 \le x \le 0.6$. Haavik et al.,[17,18] Holt et al.,[19] and Bakken et al.[20] studied the redox energetics of one end-member $SrFeO_{3-\delta}$ with adiabatic calorimetry, thermogravimetry, and coulometric titration, respectively. Other thermodynamic quantities possibly involved with cation ordering, vacancy formation, vacancy ordering, and solid solution in the brownmillerite structure, however, need to be clarified.

High-temperature oxide melt solution calorimetry is an effective tool for studying the energetics of refractory inorganic materials.[21,22] We have successfully studied the enthalpy of formation of the end-member $LaFeO_3$ along with other perovskites $LaMO_3$ (M = Cr, Co, and Ni).[23] In the current work, a large number of $La_{1-x}Sr_xFeO_{3-\delta}$ samples in the complete solid solution range $0.0 \le x \le 1.0$ were synthesized with oxygen contents confined in the ranges I−III in Figure 1, i.e., $0.0 \le \delta \le 0.5x$. Defects such as Sr'_{La}, $V_O^{\bullet\bullet}$, and $Fe^{\bullet}_{Fe}$ predominate while Fe'_{Fe} is negligible. We report enthalpies of formation from oxides and investigate the energetic trends throughout the solid solutions of $LaFeO_3-SrFeO_{2.5}$ and $LaFeO_3-SrFeO_3$. The enthalpy of oxidation of Fe^{3+} to formal Fe^{4+} is determined for each Sr composition. The enthalpy of phase transition of $SrFeO_{2.5}$ from the brownmillerite to perovskite structure at room temperature is also determined and short-range ordering of oxygen vacancies in the perovskite structure is discussed.

2. Experimental Section

2.1. Synthesis and Characterization. A suite of $La_{1-x}Sr_xFeO_{3-\delta}$ perovskites with different strontium compositions ($0.0 \le x \le 1.0$, $0.0 \le \delta \le 0.5$) was first synthesized in air either by a solid state reaction method or a liquid mix method.[24] Some portion of each sample was subsequently subjected to further heat treatment under various conditions to generate more samples with different δ values. A summary of all 36 samples and their detailed synthesis or heat treatment parameters is listed in Table 1. Each sample was conveniently denoted by a combination of its Sr content and oxygen

(13) Mizusaki, J.; Sasamoto, T.; Cannon, W. R.; Bowen, H. K. *J. Am. Ceram. Soc.* **1983**, *66*, 247.
(14) Mizusaki, J.; Yoshihiro, M.; Yamauchi, S.; Fueki, K. *J. Solid State Chem.* **1985**, *58*, 257.
(15) Kröger, F. A. *The chemistry of imperfect crystals*; North-Holland: Amsterdam, 1974; Vol. 1−3.
(16) Mizusaki, J.; Yoshihiro, M.; Yamauchi, S.; Fueki, K. *J. Solid State Chem.* **1987**, *67*, 1.
(17) Haavik, C.; Atake, T.; Kawaji, H.; Stølen, S. *Phys. Chem. Chem. Phys.* **2001**, *3*, 3863.
(18) Haavik, C.; Atake, T.; Stølen, S. *Phys. Chem. Chem. Phys.* **2002**, *4*, 1082.
(19) Holt, A.; Norby, T.; Glenne, R. *Ionics* **1999**, *5*, 434.
(20) Bakken, E.; Stolen, S.; Norby, T.; Glenne, R.; Budd, M. *Solid State Ionics* **2004**, *167*, 367.
(21) Navrotsky, A. *Phys. Chem. Miner.* **1977**, *2*, 89.
(22) Navrotsky, A. *Phys. Chem. Miner.* **1997**, *24*, 222.
(23) Cheng, J.; Navrotsky, A.; Zhou, X.-D.; Anderson, H. U. *J. Mater. Res.*, in press.
(24) Eror, N. G.; Anderson, H. U. *Mater. Res. Soc. Symp. Proc.* **1986**, *73*, 571.

Table 1. Synthesis and Phase Identification of $La_{1-x}Sr_xFeO_{3-\delta}$ Samples

x	$3-\delta$[a]	sample code	phase[b]	source	synthesis/treatment conditions
0	3.00	$LaFeO_3$	P	UCD	SSR, in air, 1400 °C/48 h
0.1	3.00	L10SF3.0	P	UCD	SSR, in air, 1300 °C/48 h
	2.95	L10SF2.95	P	UCD	from L10SF3.0, TG in 1% H_2,, 450 °C/0.5 h
0.2	3.00	L20SF3.0	P	UMR	liquid mix method
	2.94	L20SF2.94	P	UCD	from L20SF3.0, TG in Ar, 1000 °C
	2.90	L20SF2.90	P	UCD	from L20SF3.0, TG in 1% H_2, 450 °C/0.5 h
0.3	3.00	L30SF3.0	P	UCD	SSR, in air, 1230 °C/48 h
	2.85	L30SF2.85	P	UCD	from L30SF3.0, TG in 1% H_2, 550 °C/0.5 h
0.4	3.00	L40SF3.0[c]	P	UMR	liquid mix method
	2.95	L40SF2.95	P	UCD	from L40SF2.80, TG in O_2, 1000 °C
	2.88	L40SF2.88	P	UMR	liquid mix method
	2.80	L40SF2.80	P	UMR	liquid mix method, quenched from 1500 °C
				UCD	from L40SF2.80, TG in 1% H_2, 500 °C/1 h
0.5	3.00	L50SF3.0	P	UCD	SSR, in air, 1300 °C/48 h
	2.89	L50SF2.89	P	UCD	from L50SF3.0, TG in 1% H_2, 450 °C/0.5 h
	2.82	L50SF2.82	P	UCD	from L50SF3.0, TG in Ar, 1000 °C
	2.75	L50SF2.75	P	UCD	from L50SF3.0, TG in 1% H_2, 550 °C/0.5 h
0.6	3.00	L60SF3.0	P	UMR	liquid mix method
	2.70	L60SF2.70	P	UCD	from L60SF3.0, TG in 1% H_2, 500 °C/1 h
0.67	3.00	L67SF3.0	P	UMR	liquid mix method
	2.71	L67SF2.71	P	UCD	from L67SF3.0, TG in Ar, 1000 °C
0.7	3.00	L70SF3.0	P	UCD	from L70SF2.97, TG in O_2, 350 °C/1h
	2.97	L70SF2.97	P	UCD	SSR, in air, 1230 °C/48 h
	2.93	L70SF2.93	P	UCD	from L70SF2.97, quenched in air from 815 °C
	2.80	L70SF2.80	P	UCD	from L70SF3.0, TG in 1%H_2, 500 °C/0.5 h
	2.70	L70SF2.70	P	UCD	from L70SF2.97, TG in Ar, 1000 °C
	2.65	L70SF2.65	P	UCD	from L70SF3.0, TG in 1%H_2, 550 °C/1 h
0.8	2.98	L80SF2.98	P	UCD	from L80SF2.96, TG in O_2, 370 °C/1 h
	2.96	L80SF2.96[c]	P	UCD	SSR, in air, 1230 °C/48 h
	2.76	L80SF2.76	P	UCD	from L80SF2.96, TG in Ar, 700 °C
	2.60	L80SF2.60	P	UCD	from L80SF2.96, TG in 1%H_2, 500 °C/1 h
0.9	2.94	L90SF2.94	P	UCD	from L90SF2.90, TG in O_2, 370 °C/80 min
	2.90	L90SF2.90[c]	P	UMR	liquid mix method
	2.71	L90SF2.71	P	UCD	from L90SF2.90, TG in Ar, 700 °C
	2.60	L90SF2.60	P	UCD	from L90SF2.90, TG in Ar, 1000 °C
	2.55	L90SF2.55	B	UCD	from L90SF2.90, TG in 1%H_2, 500 °C/1 h
1.0	2.50	$SrFeO_{2.50}$	B	UCD	from $SrFeO_{2.80}$ (UMR), TG in 1%H_2, 500 °C/1 h

[a] Oxygen content was determined either by TG or titration. Uncertainty is ±0.01. [b] P = perovskite type, B = brownmillerite type. [c] Oxygen content was cross-checked by TG and titration.

content. For instance, for 40 mol % Sr-doped $LaFeO_3$ with oxygen deficiency of 0.12, the sample is coded as L40SF2.88.

The conventional solid-state reaction method (SSR) started with La_2O_3, Fe_2O_3, and $SrCO_3$ (purity > 99.99%, La_2O_3 from Aldrich, others from Alfa Aesar). As-received La_2O_3 powder was dried under vacuum at 800 °C and weighed in an Ar-filled glovebox. Powders with the proper cation ratio were mixed thoroughly in an alumina mortar and pressed into disks for precalcination at 1000 °C for 12 h. The heat-treated disks were then crushed and ground. The powder was pelletized under a uniaxial pressure of 25 MPa and was sintered in air at 1230−1400 °C. All samples were furnace-cooled to room temperature. Grinding, pelletizing, and sintering were repeated on each sample to ensure complete reaction.

The low-temperature liquid mix method started with La, Fe, and Sr nitrates (all from Alfa Aesar). The water content in each salt was checked by thermogravimetric decomposition experiments before using. Stoichiometric amounts of salts were dissolved in deionized water in a beaker which sat on a heating/stirring plate. Stirring was essential to ensure complete dissolution and homogeneous distribution of cations. An appropriate amount of citric acid (1 equiv of citric acid per equiv of cation) was added to the clear solution to allow chelating. The solution was slowly heated to 90 °C. Adding ethylene glycol produced polyesterification. Evaporation continued until a solid spongy polymeric resin formed. This precursor was then transferred to an alumina boat in a box furnace and slowly heated to 400 °C for 5 h for complete decomposition of organic species. The resulting black ash was ground into powder, pelletized, and calcined between 1200 and 1500 °C in air for 40 h. Samples were cooled at the rate of 3 °C/min to obtain high oxygen content or quenched in air for large oxygen nonstoichiometry.

The oxygen content in each sample was determined by thermogravimetry (TG) and/or iodometric titration (Table 1). Selected samples (L40SF3.0, L80SF2.96, and L90SF2.90) were cross-checked with these two independent methods.

Iodometric titration was carried out to directly determine the concentration of Fe^{4+} ions. The samples, which weighed 0.1−0.2 g, were completely and homogeneously dissolved in HCl and KI under an inert gas atmosphere to prevent the oxidation of I^- ions in air. The solution was then titrated with standard thiosulfate solution. The procedures were repeated three times for each sample to get an average value. Oxygen nonstoichiometry, δ, was thus calculated based on the defect model described above.

Oxygen nonstoichiometry strongly depends on the oxygen partial pressure and the temperature, which can be well-controlled in a thermogravimetric apparatus. TG analysis coupled with differential scanning calorimetry (DSC) was performed on a Netzsch STA 449 from room temperature to 1000 °C. Analyses were conducted using the software supplied by the manufacturer after continuous runs of the baseline and sample. About 80 mg of sample was pelletized to ensure good thermal contact with the Pt crucible and was heated at 10 °C/min in a specified atmosphere with a flow rate of 40 mL/min. A gas mixture of 1% H_2 and 99% Ar was found to be reducing enough for all samples, when heated to 450−550 °C and kept isothermal for 0.5−1 h, to lose oxygen to reach the plateau of Region III ($\delta = 0.5x$) in Figure 1. Samples with maximally reduced oxygen content in this study, generally written as $La_{1-x}Sr_xFeO_{3-0.5x}$, were thus obtained. The oxygen content in the sample before TG

Table 2. Thermochemical Cycles for Calculation of the Enthalpy of Drop Solution of SrO in $2PbO{\cdot}B_2O_3$ (Cycle 1) and the Enthalpies of Formation from Oxides for $La_{1-x}Sr_xFeO_{3-\delta}$ Perovskites (Cycle 2) at Room Temperature

reaction	ΔH
Cycle 1: Enthalpy of Drop Solution of SrO	
$SrCO_3$(xl, 25 °C) → SrO(sol, 702 °C) + CO_2(g, 702 °C)[a]	$\Delta H(1) = \Delta H_{DS}(SrCO_3)$
CO_2(g, 25 °C) → CO_2(g, 702 °C)	$\Delta H(2) = \Delta H_{25-702}(CO_2)$[b]
SrO(xl, 25 °C) + CO_2(g, 25 °C) → $SrCO_3$(xl, 25 °C)	$\Delta H(3) = \Delta H^{\circ}_{f,ox}(SrCO_3)$[c]
SrO(xl, 25 °C) → SrO(sol, 702 °C)	$\Delta H(4) = \Delta H_{DS}(SrO)$
$\Delta H(4) = \Delta H(1) - \Delta H(2) + \Delta H(3)$	
Cycle 2: Enthalpy of Formation of $La_{1-x}Sr_xFeO_{3-\delta}$ from Oxides	
La_2O_3(xl, 25 °C) → La_2O_3(sol, 702 °C)	$\Delta H(5) = \Delta H_{DS}(La_2O_3)$
Fe_2O_3(xl, 25 °C) → Fe_2O_3(sol, 702 °C)	$\Delta H(6) = \Delta H_{DS}(Fe_2O_3)$
SrO(xl, 25 °C) → SrO(sol, 702 °C)	$\Delta H(4) = \Delta H_{DS}(SrO)$
O_2(g, 25 °C) → O_2(g, 702 °C)	$\Delta H(7) = \Delta H_{25-702}(O_2)$[d]
$La_{1-x}Sr_xFeO_{3-\delta}$(xl, 25 °C) → $0.5(1-x)La_2O_3$(sol, 702 °C) + $0.5Fe_2O_3$(sol, 702 °C) + xSrO(sol, 702 °C) + $(0.25x - 0.5\delta)O_2$(g, 702 °C)	$\Delta H(8) = \Delta H_{DS}(La_{1-x}Sr_xFeO_{3-\delta})$
$0.5(1-x)La_2O_3$(xl, 25 °C) + $0.5Fe_2O_3$(xl, 25 °C) + xSrO(xl, 25 °C) + $(0.25x - 0.5\delta)$ O_2(g, 25 °C) → $La_{1-x}Sr_xFeO_{3-\delta}$(xl, 25 °C)	$\Delta H(9) = \Delta H^{\circ}_{f,ox}(La_{1-x}Sr_xFeO_{3-\delta})$
$\Delta H(9) = 0.5(1-x)\,\Delta H(5) + 0.5\,\Delta H(6) + x\,\Delta H(4) + (0.25x - 0.5\delta)\,\Delta H(7) - \Delta H(8)$	

[a] xl = crystalline solid, g = gas, sol = solution in $2PbO{\cdot}B_2O_3$. [b] Heat content of CO_2 from 25 °C to 702 °C, calculated from Robie and Hemingway,[26] 32.05 kJ/mol. [c] Enthalpy of formation of $SrCO_3$ from oxides at 25 °C, calculated from Robie and Hemingway,[25] −233.90 ± 1.81 kJ/mol. [d] Heat content of O_2 from 25 °C to 702 °C, calculated from Robie and Hemingway,[26] 21.84 kJ/mol.

was calculated and was compared with the value obtained from the titration. The agreement was excellent, e.g., the oxygen content in L40SF3.0, L80SF2.96, and L90SF2.90, which were determined by TG, was 2.99 ± 0.01, 2.96 ± 0.02, and 2.89 ± 0.01, respectively, from the titration measurements.

Since high-temperature solution calorimetry only requires a small amount of sample (~80 mg) and TG provides accurate measurement of the oxygen content, additional samples were conveniently synthesized in situ by TG through varying oxygen partial pressures (pure O_2, pure Ar, and 1% H_2) and temperatures (350−1000 °C). For example, L20SF3.0 was partially reduced to L20SF2.94 in Ar when heated to 1000 °C, and fully reduced to L20SF2.90 in 1% H_2 at 450 °C for 0.5 h, while L70SF2.97 could be oxidized to L70SF3.0 in O_2 at 350 °C for 1 h (Table 1).

Phase identification was carried out by powder X-ray diffraction (XRD) using a Scintag PAD V diffractometer (Cu Kα radiation) operated at 45 kV and 40 mA, with a 0.02° step size and 2−10 s dwell time.

A Cameca SX-100 electron microprobe was used for qualitative chemical analysis for powder samples. Homogeneity and impurity content were examined by X-ray dot mapping and backscattered electron images. Quantitative determination of oxygen is difficult because the oxygen content is likely to change when the sample is densified at high temperatures. However, the cation ratios obtained by microprobe are reliable.

2.2. High-Temperature Oxide Melt Solution Calorimetry. High-temperature drop solution calorimetry was performed for all $La_{1-x}Sr_xFeO_{3-\delta}$ samples in a Tian-Calvet twin microcalorimeter using lead borate ($2PbO{\cdot}B_2O_3$) as the solvent at 702 °C. Details of the equipment and experimental procedures have been described elsewhere.[21,22] Calibration of the calorimeter was based on the heat content of ~5 mg of corundum pellets as a standard laboratory protocol. Argon was flushed through the calorimeter assembly (40 mL/min) to blow out any gas species evolved in the calorimeter. The solvent was agitated by bubbling argon gas through it (5 mL/min) to facilitate dissolution and prevent local saturation.

A reproducible final oxidation state of the iron dissolved in the lead borate solvent is crucial to interpreting the calorimetric data. The final state of Fe ions for Fe^{3+}-containing samples (e.g., Fe_2O_3 and $LaFeO_3$) was determined by both weight loss experiments and drop solution calorimetry to be 3+, regardless of the local atmosphere (Ar or O_2) in the solvent.[23,25] The final state of Fe ions in lead borate for both Fe^{3+} and Fe^{4+}-containing samples, i.e., $La_{1-x}Sr_xFeO_{3-\delta}$ ($\delta < 0.5x$), was determined by weight loss measurements as follows. L40SF3.0 of known weight was added to lead borate which had been previously equilibrated at 700 °C to constant weight in a platinum crucible. The mixture was heated at 702 °C in air for 60 min, which mimicked the duration of a drop solution experiment, and cooled to room temperature. The weight was measured again and any difference was attributed to oxygen loss. The measured weight loss showed that iron dissolves in lead borate as Fe^{3+}, with any formal Fe^{4+} evolving oxygen gas upon dissolution.

Drop solution calorimetry (DS) involves dropping a sample pellet from room temperature (25 °C) into the molten solvent in the calorimeter at 702 °C. For samples with virtually no Fe^{4+} present, the total heat effect, enthalpy of drop solution (H_{DS}), is equal to the heat of solution at 702 °C plus the heat content from 25 to 702 °C. For samples containing Fe^{4+}, the heat effect associated with the reduction of Fe^{4+} to Fe^{3+} is included in the enthalpy of drop solution.

SrO is too hygroscopic to be prepared and handled easily. Its enthalpy of drop solution was calculated from the enthalpy of drop solution of $SrCO_3$ and other related thermodynamic data using the first thermochemical cycle in Table 2. The enthalpies of formation from oxides for the $La_{1-x}Sr_xFeO_{3-\delta}$ samples were calculated using the second thermochemical cycle in Table 2.

3. Results and Discussion

3.1. Samples and Structure Determination. The oxygen content in each $La_{1-x}Sr_xFeO_{3-\delta}$ sample, $3-\delta$, depends on the doping level of Sr, oxygen partial pressure, annealing temperature, and cooling rate (Table 1). Using thermogravimetry, oxygen nonstoichiometry analyses were coupled with the syntheses of those oxygen-deficient samples in reducing atmospheres or oxygen-rich samples in oxidizing atmospheres. Titration on several selected samples confirmed

(25) Brown, N. E.; Navrotsky, A. *Am. Mineral.* **1994**, *79*, 485.
(26) Robie, R. A.; Hemingway, B. S. *Thermodynamic properties of minerals and related substances at 298.15 K and 1 Bar (10^5 Pascals) pressure and at higher temperatures*; U.S. Geological Survey Bulletin, No. 2131; Washington D.C., 1995.

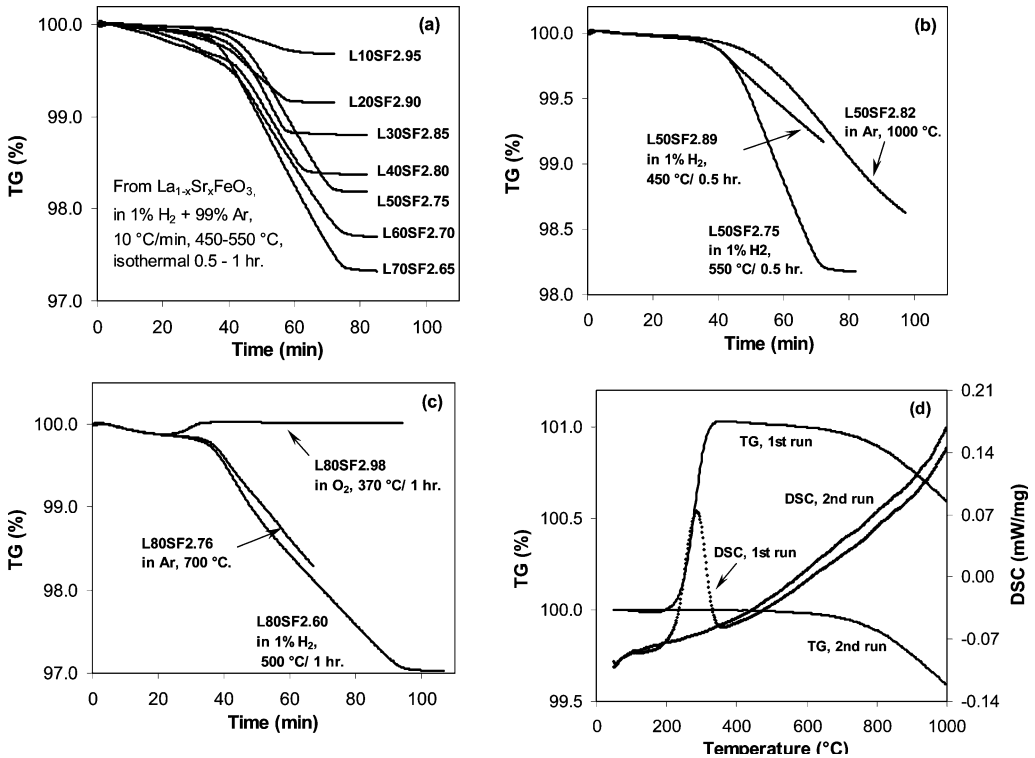

Figure 2. TG/DSC curves indicating oxygen nonstoichiometry in $La_{1-x}Sr_xFeO_{3-\delta}$ samples ($0.0 \le x < 1.0$ and $0 \le \delta \le x/2$) as functions of oxygen partial pressure and temperature. (a) Fully oxidized perovskites ($x = 0.1$ to 0.7, $\delta = 0$) were reduced to $\delta = 0.5x$. (b) In situ syntheses of the series of L50SF samples from L50SF3.0. (c) In situ syntheses of the series of L80SF samples from L80SF2.96. (d) Oxygen absorption of L40SF2.80 in an oxygen atmosphere and the enthalpy of absorption associated with it.

the values of oxygen content obtained by TG. Examples of TG/DSC curves are shown in Figure 2. A total weight loss of no more than 0.1 wt % below 200 °C for each sample was assigned to desorption of a small amount of surface water.

The TG results in Figure 2a show that samples with the compositions of $0.1 \le x \le 0.7$ and presumably having the highest oxygen contents, when treated in 1% H_2 at 450−550 °C, lost weight to reach equilibrium. The weight loss equals the loss of oxygen from 3 to $3 - 0.5x$ in each sample. Figures 2b and 2c are two examples, L50SF and L80SF, of the in situ syntheses of samples with different oxygen contents by tuning heat treatment parameters. For each Sr composition, with decreasing oxygen partial pressure (in the order of pure oxygen, air, pure Ar, and 1% H_2) and increasing temperature, more oxygen vacancies are formed at the expense of Fe^{4+} ions. Figure 2d illustrates two consecutive TG/DSC runs of L40SF2.80 in oxygen at 25−1000 °C. In the first run, oxygen absorption occurs quickly at 200−350 °C and oxygen content remains constant until ∼700 °C. The second run proves that the oxygen loss between 700 and 1000 °C is reversible. The weight gain of oxygen after the first run corresponds to a new sample with the formula of L40SF2.95. The area under the peak of the first DSC run represents the enthalpy of oxygen absorption.

As seen in Table 1, for samples with $x \le 0.67$ prepared in air using furnace cooling, oxygen deficiency is essentially zero. This is consistent with the observations of Mizusaki et al.[14] For samples of $x \ge 0.7$ synthesized in air, the full oxygen content of 3 cannot be obtained. The higher the Sr composition, the larger the oxygen deficiency. Higher oxygen content can be achieved by annealing the samples under pure oxygen; e.g., L70SF2.97 was oxidized to L70SF3.0 and L80SF2.96 to L80SF2.98 (Figure 2c).

All 36 samples were confirmed to be single phase at ambient temperature by powder XRD and to be homogeneous on the micrometer scale by electron microprobe analysis. Two fully reduced samples, L90SFO2.55 ($La_{0.1}Sr_{0.9}FeO_{2.55}$) and the end-member $SrFeO_{2.5}$, were found to possess the brownmillerite-type structure, while all other samples have the perovskite structure.

The undoped perovskite structure with the general formula ABO_3 is a corner-sharing three-dimensional framework of BO_6 octahedra with A cations occupying the cavity sites. Doping, on the A site or the B site or both, not only modifies the physical properties such as conduction in $La_{1-x}Sr_xFeO_{3-\delta}$ but also distorts the perovskite structure. A brownmillerite structure ($ABO_{2.5}$) is derived from the parent cubic perovskite structure by creating lines of oxygen vacancies along the $[101]_p$ direction in every other $(010)_p$ plane. Consequently, the structure contains alternate stacks of planes composed of BO_6 octahedra and planes composed of BO_4 tetrahedra.[27] It can also be considered an orthorhombic perovskite with long-range ordered oxygen vacancies. The solubility of Sr in a $LaFeO_3$ perovskite system is large (0−0.9) while the La in $SrFeO_{2.5}$ brownmillerite system is rather small (0−0.1). We see no evidence for a two-phase region, brownmillerite plus perovskite.

The assignment of a space group and the determination of detailed structural parameters for $La_{1-x}Sr_xFeO_{3-\delta}$ are complicated by the Sr doping amount and the oxygen

(27) Mizusaki, J.; Okayasu, M.; Yamauchi, S.; Fueki, K. *J. Solid State Chem.* **1992**, *99*, 166.

Table 3. Enthalpies of Drop Solution (ΔH_{DS}) of Oxides and $La_{1-x}Sr_xFeO_{3-\delta}$ Perovskites in $2PbO{\cdot}B_2O_3$ at 702 °C and Enthalpies of Formation of Perovskites from Oxides ($\Delta H_{f,ox}$) at 25 °C

	sample	ΔH_{DS} (kJ/mol)	$\Delta H_{f,ox}$ (kJ/mol)		sample	ΔH_{DS} (kJ/mol)	$\Delta H_{f,ox}$ (kJ/mol)
	La_2O_3	-43.11 ± 4.5[a]		0.6	L60SF3.0	107.07 ± 0.43 (9)	-61.96 ± 1.65
	Fe_2O_3	170.59 ± 1.29[b]			L60SF2.70	84.09 ± 1.60 (8)	-42.26 ± 2.26
	$SrCO_3$	207.88 ± 0.50 (8)[c]		0.67	L67SF3.0	105.82 ± 0.89 (9)	-62.78 ± 1.84
	SrO	-58.07 ± 1.90			L67SF2.71	84.07 ± 1.11 (8)	-44.24 ± 1.96
$x = 0$	$LaFeO_3$	127.87 ± 1.26 (9)	-64.13 ± 2.68	0.7	L70SF3.0	109.30 ± 0.74 (8)	-67.29 ± 1.79
0.1	L10SF3.0	121.73 ± 1.25 (11)	-61.10 ± 2.49		L70SF2.97	107.25 ± 0.75 (8)	-65.53 ± 1.79
	L10SF2.95	116.54 ± 1.74 (9)	-56.45 ± 2.77		L70SF2.93	104.59 ± 0.97 (8)	-63.35 ± 1.89
0.2	L20SF3.0	119.72 ± 0.82 (9)	-62.19 ± 2.13		L70SF2.80	92.11 ± 1.03 (7)	-52.30 ± 1.92
	L20SF2.94	112.59 ± 0.63 (9)	-55.71 ± 2.06		L70SF2.70	84.59 ± 0.95 (7)	-45.86 ± 1.88
	L20SF2.90	108.87 ± 1.04 (8)	-52.44 ± 2.22		L70SF2.65	79.23 ± 0.57 (8)	-41.05 ± 1.72
0.3	L30SF3.0	118.15 ± 1.70 (11)	-63.73 ± 2.48	0.8	L80SF2.98	107.65 ± 0.69 (10)	-68.97 ± 1.85
	L30SF2.85	100.11 ± 0.93 (8)	-47.33 ± 2.03		L80SF2.96	105.17 ± 0.71 (9)	-66.71 ± 1.85
0.4	L40SF3.0	114.96 ± 1.37 (14)	-63.64 ± 2.17		L80SF2.76	90.16 ± 2.55 (6)	-53.89 ± 3.07
	L40SF2.95	110.21 ± 0.62 (8)	-59.44 ± 1.80		L80SF2.60	74.12 ± 1.24 (7)	-39.59 ± 2.10
	L40SF2.88	101.59 ± 1.24 (10)	-51.58 ± 2.10	0.9	L90SF2.94	101.41 ± 1.06 (8)	-66.27 ± 2.13
	L40SF2.80	95.35 ± 1.33 (11)	-46.21 ± 2.15		L90SF2.90	97.54 ± 0.74 (8)	-62.84 ± 1.99
		95.25 ± 1.16 (4)[d]					
0.5	L50SF3.0	112.34 ± 1.23 (14)	-64.12 ± 2.03		L90SF2.71	83.72 ± 1.80 (8)	-51.10 ± 2.57
	L50SF2.89	100.99 ± 1.38 (9)	-53.98 ± 2.12		L90SF2.60	74.16 ± 1.00 (6)	-42.74 ± 2.10
	L50SF2.82	95.18 ± 1.74 (9)	-48.93 ± 2.37		L90SF2.55	70.37 ± 1.66 (6)	-39.49 ± 2.48
	L50SF2.75	87.63 ± 0.91 (8)	-42.15 ± 1.86	1.0	SrFeO2.50	73.83 ± 1.71 (9)	-46.60 ± 2.36

[a] From Cheng and Navrotsky.[33] [b] From Majzlan et al.[34] [c] Uncertainty is two standard deviations of the mean; number in ( ) is the number of experiments. [d] Data for L40SF2.80 were prepared at UCD and were the same within error as the value for the one from UMR.

Table 4. Thermochemical Cycle for Calculation of the Enthalpy of Oxidation (ΔH_{oxid}) between Two $La_{1-x}Sr_xFeO_{3-\delta}$ Samples Which Only Differ in Oxygen Contents (Assuming $\delta' > \delta$)

reaction	ΔH
$La_{1-x}Sr_xFeO_{3-\delta'}$(xl, 25 °C) → $0.5(1-x)La_2O_3$(sol, 702 °C) + $0.5Fe_2O_3$(sol, 702 °C) + xSrO(sol, 702 °C) + $(0.25x - 0.5\delta')O_2$(g, 702 °C)	$\Delta H(10) = \Delta H_{DS}(La_{1-x}Sr_xFeO_{3-\delta'})$
$La_{1-x}Sr_xFeO_{3-\delta}$(xl, 25 °C) → $0.5(1-x)La_2O_3$(sol, 702 °C) + $0.5Fe_2O_3$(sol, 702 °C) + xSrO(sol, 702 °C) + $(0.25x - 0.5\delta)O_2$(g, 702 °C)	$\Delta H(11) = \Delta H_{DS}(La_{1-x}Sr_xFeO_{3-\delta})$
O_2(g, 25 °C) → O_2(g, 702 °C)	$\Delta H(7) = \Delta H_{25-702}(O_2)$
$La_{1-x}Sr_xFeO_{3-\delta'}$(xl, 25 °C) + $0.5(\delta'-\delta)$ O_2(g, 25 °C) → $La_{1-x}Sr_xFeO_{3-\delta}$(xl, 25 °C)	$\Delta H(12) = \Delta H_{oxid}$ from $3-\delta'$ to $3-\delta$
$\Delta H(12) = \Delta H(10) - \Delta H(11) + 0.5(\delta'-\delta)\,\Delta H(7)$	

nonstoichiometry. In fact, the phase relations at both low temperatures and elevated temperatures are not well-established and sometimes are controversial. Complex phase variations have been extensively studied by XRD, neutron diffraction, and Mössbauer spectroscopy.[28−31] For example, in the $La_{1-x}Sr_xFeO_{3-\delta}$ system with δ close to zero, structures changed from orthorhombic at low x ($0 \le x \le 0.2$) through rhombohedral ($0.4 \le x \le 0.7$) to cubic at high x ($0.8 \le x \le 1.0$).[28] For a given x, e.g., L67SF, the phases changed from cubic to tetragonal to orthorhombic when oxygen content decreased from 3 to 2.67.[29] In both studies, it was also proposed that a mixture of two perovskite structures for some particular composition may exist.[28,29] Furthermore, even for a single phase determined by powder XRD, the possibility cannot be ruled out that it actually consists of intergrowths at the nanoscale of closely related perovskite phases due to interactions among defects.[4]

In this study, therefore, we do not pursue the refinement of each sample's structure, but instead, highlight the effects of defect chemistry on their thermodynamic properties. This approach was also used in the studies by Mizusaki et al.[14,16] The effect of these symmetry changes on the energetics is probably small (<1 kJ/mol) as seen for other perovskites.[32]

3.2. Enthalpies of Formation from Oxides. Nominal compositions were used in the thermochemical cycle (Table 2) to calculate the enthalpies of formation from oxides for all the $La_{1-x}Sr_xFeO_{3-\delta}$ samples. The enthalpies of drop solution of constituent oxides (La_2O_3, Fe_2O_3, and SrO) and $La_{1-x}Sr_xFeO_{3-\delta}$ samples and the corresponding enthalpies of formation from oxides at room temperature are summarized in Table 3. The exothermic formation enthalpies show the stability of each sample with respect to its component oxides.

It is worth noting that, in Tables 1 and 3, the enthalpy of drop solution for one L40SF2.80 sample, which was prepared from quenching, was in excellent agreement with that for another L40SF2.80 obtained from TG treatment. This further verified the usefulness of TG as a sample preparation method.

The enthalpies of formation in the $La_{1-x}Sr_xFeO_{3-\delta}$ system can be modeled by several competing energetic factors: (a) enthalpy of oxygen vacancy formation involving Sr substitution (without oxidation); (b) enthalpy of oxidation of Fe^{3+} to formal Fe^{4+} (oxygen vacancy filling); (c) effects of cation ordering, i.e., Sr and La on A site and Fe^{3+} and Fe^{4+} on B site; (d) effects of oxygen vacancy ordering on anionic sublattices; and (e) effects of structural phase transitions within distorted perovskite structures or between perovskite and brownmillerite.

(28) Dann, S. E.; Currie, D. B.; Weller, M. T. *J. Solid State Chem.* **1994**, *109*, 134.
(29) Battle, P. D.; Gibb, T. C.; Nixon, S. *J. Solid State Chem.* **1989**, *79*, 75.
(30) Schmidt, M.; Campbell, S. J. *J. Solid State Chem.* **2001**, *156*, 292.
(31) Takeda, Y.; Kanno, K.; Takada, T.; Yamamoto, O.; Takano, M.; Nakayama, N.; Bando, Y. *J. Solid State Chem.* **1986**, *63*, 237.
(32) Cheng, J.; Navrotsky, A. *J. Solid State. Chem.* 2004, *177*, 126.

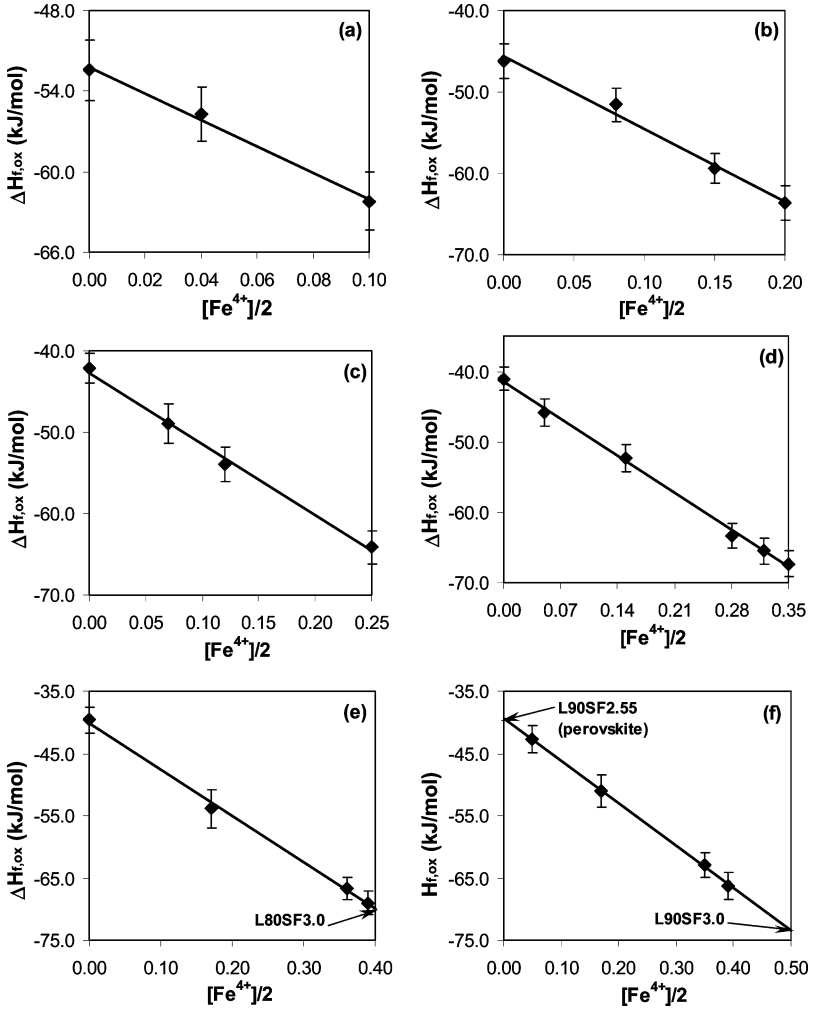

Figure 3. Enthalpy of formation vs oxygen nonstoichiometry in each $La_{1-x}Sr_xFeO_{3-\delta}$ series with a given x. (a) L20SF; (b) L40SF; (c) L50 SF; (d) L70SF; (e) L80SF; and (f) L90SF. The enthalpies of formation of fully oxidized L80SF3.0 and L90SF3.0, and maximally reduced L90SF2.55 (with perovskite structure) were estimated from the linear extrapolation in (e) and (f). The slope in each plot represents the enthalpy of oxidation (ΔH_{oxid}, in kJ/mol O_2).

3.3. Enthalpy of Oxidation. For each $La_{1-x}Sr_xFeO_{3-\delta}$ series with a given x ($0 < x < 1.0$), different oxygen contents between maximum ($\delta = 0$) and minimum ($\delta = 0.5x$) were achieved through thermal treatment. For all samples we adopt the point defect model assuming the formal valence states of Fe would be 3+ and/or 4+ and without implying any microscopic picture of partial oxidation state, band occupancy, or covalency. Thus, the enthalpy of oxidation (ΔH_{oxid}) between two samples is determined by the thermochemical cycle shown in Table 4 and represents the enthalpy change of the reaction

$$La_{1-x}Sr_xFeO_{3-\delta'}(xl, 25\ °C) + 0.5(\delta' - \delta) \times O_2(g, 25\ °C) \rightarrow La_{1-x}Sr_xFeO_{3-\delta}(xl, 25\ °C) \quad (4)$$

This approach is similar to that used earlier in calorimetric studies of alkaline earth-doped K_2NiF_4-type La_2MO_4 (M = Cu, Co, Ni) oxides.[35−37]

One example is the oxidation of L40SF2.80 to L40SF2.95. The heat of oxidation is calculated as -13.23 ± 1.47 kJ/mol using their enthalpies of drop solution and the correction for the heat content of oxygen (Table 4). This value is in excellent agreement with that obtained from the DSC measurement in Figure 2d, that is, the area under the DSC peak, -13.24 ± 0.40 kJ/mol. Unfortunately, this DSC method is not applicable to all samples for measuring the enthalpy of oxidation because the oxygen difference between any two given samples ($\delta' - \delta$) is not necessarily equal to the oxygen gain under the DSC conditions after equilibrium.

The enthalpy of oxidation (reaction) could be a function of Sr doping amount (x) and oxygen deficiency (δ). First, we plot the enthalpies of formation from oxides vs the concentration of formal Fe^{4+} ($[Fe^{4+}]/2 = -\delta$) in each $La_{1-x}Sr_xFeO_{3-\delta}$ series ($0 < x < 1.0$) with perovskite-type structure. Some examples are shown in Figure 3. An approximately linear relationship can be found in each plot, implying that the enthalpy of oxidation in each series is virtually independent of the oxygen content. The slope of each line represents the normalized enthalpy of oxidation in kJ/(mol oxygen atom), which is often converted to kJ/mol

(33) Cheng, J.; Navrotsky, A. *J. Mater. Res.* **2003**, *18*, 2501.
(34) Majzlan, J.; Navrotsky, A.; Evans, B. *J. Phys. Chem. Miner.* **2002**, *29*, 515.
(35) Bularzik, J.; Navrotsky, A.; DiCarlo, J.; Bringley, J.; Scott, B.; Trail, S. *J. Solid State Chem.* **1991**, *94*, 418.
(36) DiCarko, J.; Mehta, A.; Banschick, D.; Navrotsky, A. *J. Solid State Chem.* **1993**, *103*, 186.
(37) Prasanna, T. R. S.; Navrotsky, A. *J. Solid State Chem.* **1994**, *112*, 192.

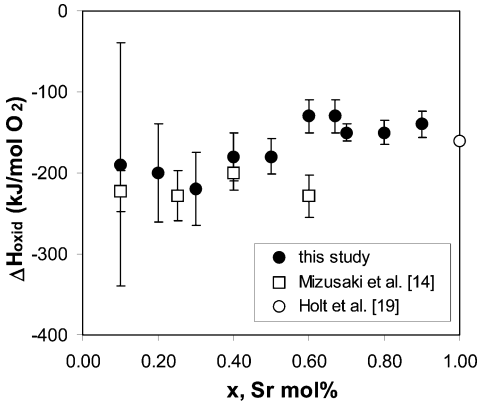

Figure 4. Enthalpy of oxidation (ΔH_{oxid}, in kJ/mol O_2) in the $La_{1-x}Sr_xFeO_{3-\delta}$ system as a function of Sr content (x). Data from literature studies are also included. (●, this study, at room temperature; ○, Mizusaki et al.[14] at 600−1000 °C; □, Holt et al.[19] at 750−1200 °C.)

O_2 for convenience. For instance, the average enthalpy of oxidation in L40SF series is -180 ± 30 kJ/mol O_2.

Using linear extrapolation or interpolation in each plot, the enthalpy of formation for any composition with perovskite structure can be obtained. Of interest for this study are three high Sr doping level perovskite samples, L80SF3.0, L90SF3.0, and L90SF2.55, which are not experimentally available. The values are -69.81 ± 3.25, -70.02 ± 4.10, and -39.35 ± 2.20 kJ/mol, respectively.

The normalized enthalpy of oxidation in each series, along with the data available in the literature,[14,19] is plotted vs Sr composition (x) in Figure 4. The uncertainty of each point reflects the standard deviation of the calorimetric measurements. While the uncertainty is quite large (>20%) for $x = 0.1-0.3$, it is ~10% for the other seven compositions with higher strontium content. One reason for this variation is the small value of difference in oxygen content ($\delta' - \delta$) for the first three compositions. The uncertainty in the enthalpy of oxidation is magnified because the difference in the enthalpy of formation of samples with the same x but different δ is small, and the difference in oxygen content ($\delta' - \delta$) is also small.

The data in Figure 4 suggest that the enthalpy of oxidation for $x = 0.1-1.0$ separates into two regimes as a first approximation: roughly constant values of -200 ± 50 kJ/mol O_2 for $x \le 0.5$ and -140 ± 30 kJ/mol O_2 for $0.5 < x < 1.0$. This means in each regime the variation of the enthalpy of oxidation with Sr composition and oxygen nonstoichiometry is small. Mizusaki et al.[14,16] determined a nearly constant value of -215 kJ/mol O_2 for $0 \le x \le 0.6$ at 600−1000 °C and assumed an ideal solution model in which point defects were randomly distributed. This value agrees, within error, with our data at room temperature for compositions ≤ 0.5. Holt et al.[19] estimated the enthalpy of oxidation for the end-member $SrFeO_{3-\delta}$ system at 750−1200 °C as -160 kJ/mol O_2, which falls within our data set for $0.5 < x < 1.0$.

The two-regime scenario may be explained as follows. The oxidation (eq 4) can be rewritten in a defect equation as

$$2Fe_{Fe}^{\times} + V_O^{\bullet\bullet} + 0.5O_2(g) = 2Fe_{Fe}^{\bullet} + O_O^{\times} \qquad (5)$$

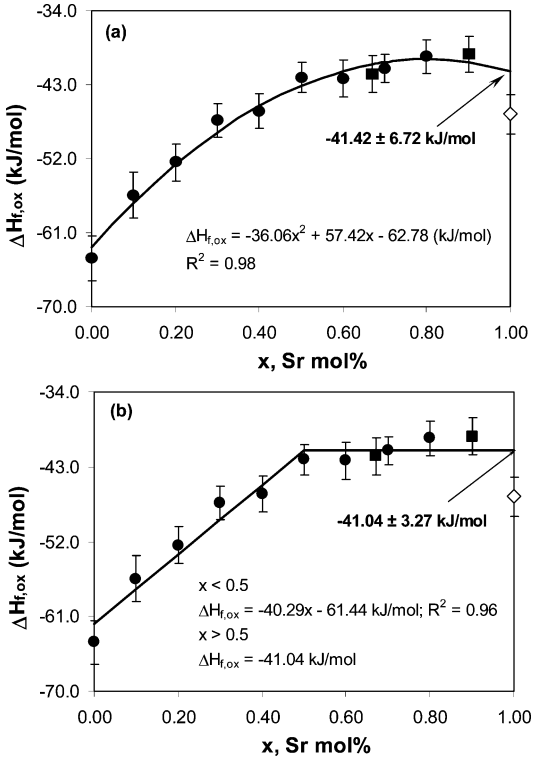

Figure 5. Enthalpy of formation from oxides for the $LaFeO_3-SrFeO_{2.5}$ solid solution system vs Sr content (x). Data are from calorimetry (solid circle) or from extrapolation (solid square). The enthalpy of formation of brownmillerite-type $SrFeO_{2.5}$ is also marked as an open symbol. (a) Quadratic fit and (b) two linear segments fit. The enthalpy of formation of perovskite-type $SrFeO_{2.5}$ derived in both fits is in reasonable agreement.

in which the oxidation of Fe^{3+} to formal Fe^{4+} is accompanied by the filling of oxygen vacancies. A more endothermic enthalpy of oxidation in the composition range of $0.5 < x \le 1$, -140 ± 30 kJ/mol O_2, compared with -200 ± 50 kJ/mol O_2 for $0 < x \le 0.5$, implies a stronger tendency to retain oxygen vacancies. This suggests oxygen vacancies may be stabilized by some means such as short-range ordering. While the random distribution of defects can model the thermodynamic properties for lower Sr doping levels ($x \le 0.5$), it is probably insufficient for $x > 0.5$. This is discussed below in relation to the formation of the brownmillerite structure.

3.4. $LaFeO_3-SrFeO_{2.5}$ Solid Solution. Based on the point defect model, no formal Fe^{4+} ions are present in the $LaFeO_3-SrFeO_{2.5}$ solution and charge balance is achieved by the required stoichiometric number of oxygen vacancies. The enthalpies of formation from oxides for the $La_{1-x}Sr_xFeO_{3-0.5x}$ series with perovskite-type structure are plotted in Figure 5. The $\Delta H_{f,ox}$ values of L67SF2.67 and L90SF2.55 perovskites are extrapolated from the plots of enthalpy of formation vs oxygen deficiency in the L67SF and L90SF series, respectively.

The enthalpy of formation from oxides for each $La_{1-x}Sr_xFeO_{3-0.5x}$ perovskite is equal to the weighted sum of the enthalpies of formation of $LaFeO_3$ and $SrFeO_{2.5}$ perovskites plus the enthalpy of mixing in the solid solution. This can be expressed as

$$\Delta H_{f,ox}(\mathrm{LSF}) = [(1-x)\Delta H_{f,ox}(LaFeO_3) + x\Delta H_{f,ox,p}(SrFeO_{2.5})] + \Delta H_{mix} \qquad (6)$$

where $\Delta H_{f,ox,p}(SrFeO_{2.5})$ is the enthalpy of formation from oxides for $SrFeO_{2.5}$ with the perovskite structure. $SrFeO_{2.5}$ is known to be isostructural with brownmillerite at ambient conditions.

Thus, the enthalpies of formation can be fitted to a function quadratic in composition shown in Figure 5a:

$$\Delta H_{f,ox}(\mathrm{LSF}) = (36.06 \pm 4.89)x^2 + (57.42 \pm 4.53)x + (-62.78 \pm 0.89)\ \mathrm{kJ/mol} \quad (7)$$

This can be recast in the form of eq 6 as

$$\Delta H_{f,ox}(\mathrm{LSF}) = [(1-x)(-62.78 \pm 0.89) + x(-41.42 \pm 6.72)] + (36.06 \pm 4.89)x(1-x)\ \mathrm{kJ/mol} \quad (8)$$

The enthalpy of formation from oxides for perovskite-type $SrFeO_{2.5}$ is therefore estimated as -41.42 ± 6.72 kJ/mol.

The term in $x(1-x)$ is reminiscent of the one-parameter regular solution model in which the heat of mixing has the form

$$\Delta H_{mix} = Wx(1-x) \quad (9)$$

where W is an interaction parameter. In this case, W, 36.1 $\pm$ 4.9 kJ/mol, is positive. Since the ionic radius of La^{3+} (0.136 nm for 12-coordinated) is quite different from Sr^{2+} (0.144 nm),[38] size mismatch results in a strong repulsive force that tends to drive phase separation, as reflected on the relatively large interaction parameter.

However, the quadratic fit does not automatically imply regular solution behavior of the $LaFeO_3-SrFeO_{2.5}$ solution with respect to perovskite end-members. The entropy of mixing cannot be of the ideal form $\Delta S_{mix} = -R[x \ln x + (1-x)\ln(1-x)]$ because there is mixing on both cation and anion sublattices (La and Sr on cation sites, oxygen ions, and vacancies on anion sites). If the mixing on both sublattices is statistically ideal, ΔS_{mix} is greater than Raoultian. But if substantial defect association occurs, ΔS_{mix} may be smaller than Raoultian.

We have studied the energetics of alkaline earth-doped $LaGaO_3$ perovskite systems,[32] in which the charge imbalance between dopant and host are exclusively compensated through the formation of oxygen vacancies. The enthalpies of formation from oxides were found to become linearly more endothermic with increasing oxygen deficiency up to the solubility limit ($\delta = 0.20$). This dramatic destabilization effect was attributed to the partial disconnection of the corner-sharing framework.[32] Similarly, an alternative way to fit the enthalpies of formation in the $LaFeO_3-SrFeO_{2.5}$ solid solution may be by two straight line segments intersecting at ~0.50 (Figure 5b). The enthalpy of formation data can be fitted by

$$\Delta H_{f,ox}(\mathrm{LSF}) = (40.29 \pm 5.47)x + (-61.44 \pm 1.84)\ \mathrm{kJ/mol} \quad \text{for } x \le 0.50$$

$$\Delta H_{f,ox}(\mathrm{LSF}) = -41.04 \pm 3.27\ \mathrm{kJ/mol} \quad \text{for } x \ge 0.50 \quad (10)$$

The perovskite $LaFeO_3-SrFeO_{2.5}$ solution is thus divided into two ranges, low Sr doping levels ($x \le 0.5$) and high Sr doping levels ($x \ge 0.5$). In the first range, the system becomes less stable with more oxygen vacancies. The oxygen deficiency is less than 0.25 and can be roughly considered as dilute, which agrees with the ideal solution model proposed by Mizusaki et al.[14,16] The slope represents the enthalpy of charge-coupled substitution involving oxygen vacancy formation which is often abbreviated as "enthalpy of vacancy formation" in kJ/mol $V_O^{\bullet\bullet}$. The enthalpy of vacancy formation is about 90 ± 11 kJ/mol $V_O^{\bullet\bullet}$ in this Sr-doped $LaFeO_3$ system. The positive sign indicates a destabilizing effect.

In the second range, the enthalpy of formation is approximately a constant. The destabilization by the oxygen vacancy formation is offset by some strong stabilizing effect such as oxygen vacancy ordering. Oxygen vacancies are concentrated and tend to order. This is consistent with the result that the enthalpy of oxidation in this concentrated range is more endothermic (−140 kJ/mol O_2) than that in the first dilute range (−200 kJ/mol O_2). Battle et al.[29] found evidence of oxygen vacancy ordering in L67SF samples using Mössbauer spectroscopy. Defect ordering was also observed in the Sr-doped $LaCoO_3$ system with high Sr contents.[4]

Extrapolating to the pure end-member $x = 1$, $\Delta H_{f,ox,p}(SrFeO_{2.5})$ is estimated from this two straight line segments model as -41.0 ± 3.3 kJ/mol. This value is the same, within uncertainty, as the one derived from the quadratic fit.

3.5. Brownmillerite−Perovskite Transition. In a brownmillerite structure ($ABO_{2.5}$), oxygen vacancies are completely ordered. Brownmillerite transforms to a defect perovskite structure at elevated temperatures. For example, the transition temperature for $BaInO_{2.5}$ is about 930 °C.[39] Phase transition in $SrFeO_{2.5}$ is complicated by the oxygen nonstoichiometry and the transition temperature is a function of oxygen partial pressure.[19,27] With careful control to keep the initial composition during heating, i.e., $SrFeO_{2.5}$, the transition temperature was determined as 830 °C by Takeda et al.[31] or 850 °C by Grenier et al.[40] Haavik et al. also determined the transition point at 847 °C.[41] Schmidt and Campbell[30] observed a broad transition peak centered at 867 °C in their differential thermal analysis (DTA) measurement of $SrFeO_{2.5}$ in a pure Ar atmosphere.

There have been only a few studies of the enthalpy associated with the phase transition. Two independent sets of DTA data were reported, 7.5 kJ/mol by Schmidt and Campbell[30] and 8.5 ± 1.2 kJ/mol by Haavik.[42] In this study we report the hypothetical enthalpy of transition at room temperature. Extrapolation to the end-member $SrFeO_{2.5}$ from Figures 5a and 5b gives the enthalpy of formation of perovskite-type $SrFeO_{2.5}$ as -41.4 ± 6.7 kJ/mol and -41.0 ± 3.3 kJ/mol, respectively. The enthalpy of formation of brownmillerite-type $SrFeO_{2.5}$ is -46.6 ± 2.4 kJ/mol (Table 3). Therefore, the enthalpy of transition of $SrFeO_{2.5}$ from the brownmillerite to perovskite modification at room

(38) Shannon, R. D. *Acta Crystallogr. A* **1976**, *32*, 751.
(39) Prasanna, T. R. S.; Navrotsky, A. *J. Mater. Res.* **1993**, *8*, 1484.
(40) Grenier, J. C.; Ea, N.; Pouchard, M.; Hagenmuller, P. *J. Solid State Chem.* **1985**, *58*, 243.
(41) Haavik, C.; Bakken, E.; Norby, T.; Stolen, S.; Atake, T.; Tojo, T. *Dalton Trans.* **2003**, 361.
(42) Haavik, C. D.Sc. Dissertation, Faculty of Mathematics and Natural Sciences, University of Oslo, 2001.

temperature is calculated as 5.5 ± 4.0 kJ/mol. The large uncertainty incorporates the standard deviations of both the calorimetric measurements and the linear fit in Figure 5b. Our value appears somewhat lower than those obtained from DTA measurement but overlaps those values when the uncertainties are considered.

The entropy of the phase transition is determined by the relation

$$\Delta S_{trans} = \Delta H_{trans}/T_{trans} \tag{11}$$

Assuming the transition occurs at 850 °C (1123 K)[40] and the enthalpy of transition is 8.5 kJ/mol,[42] ΔS_{trans} is calculated as 7.6 J/(K·mol). This value is very close to the one experimentally determined from DTA by Havvik.[42] If complete disorder of the oxygen vacancies is assumed after transition, the configurational entropy arising from the mixing of 0.5 oxygen vacancy and 2.5 oxygen per formula unit, given by the relation

$$\Delta S_{conf} = -3R\left[\frac{1}{6}\ln\frac{1}{6} + \frac{55}{66}\right] \tag{12}$$

is 11.3 J/(K·mol). The observed entropy of transition is thus somewhat smaller than the configurational entropy. This suggests that, if oxygen vacancy disordering is in fact involved in the transition, less than full randomization occurs. This in turn implies significant short-range order in the high-temperature $SrFeO_{2.5}$ phase. Similar results were reported for $BaInO_{2.5}$.[39] Our result is also consistent with the Mössbauer spectroscopic measurements by Takeda et al.[31] in which similar spectra were obtained below and above the transition temperature. This implies that local environments for most of the Fe ions remain unchanged, again an argument for short-range order. Bakken et al.[43] proposed that this short-range ordered (or long-range disordered) phase might consist of a mixture of FeO_4 tetrahedra, FeO_5 square pyramids, and FeO_6 octahedra.

The enthalpy of formation of brownmillerite-type L90SF2.55 was determined from the calorimetric measurement as −39.49 ± 2.48 kJ/mol, while that of perovskite-type L90SF2.55 was −39.35 ± 2.20 kJ/mol from the extrapolation in Figure 3f. So the enthalpy of transition of L90SF2.55 from the brownmillerite to perovskite structure is essentially zero. With less Sr doping, e.g., in L80SF2.60, long-range oxygen vacancy ordering is no longer energetically favorable. But as expected, extensive short-range ordering still prevails, possibly until $x = 0.5$. Ordering then diminishes when $x < 0.5$. So the two linear line segments fit in Figure 5 may have more physical meaning than the quadratic fit.

3.6. $LaFeO_3$-$SrFeO_3$ Solid Solution. In the $La_{1-x}Sr_xFeO_3$ solid solution, charge imbalance is all compensated by the oxidation of Fe^{3+} to formal Fe^{4+} and no oxygen vacancies are present. Every sample has the perovskite structure, though some are distorted. The enthalpies of formation from oxides are plotted in Figure 6. The $\Delta H_{f,ox}$ values of L80SF3.0 and L90SF3.0 are extrapolated from the plots of enthalpy of formation vs oxygen deficiency in L80SF and L90SF series, respectively (Figures 3e and 3f).

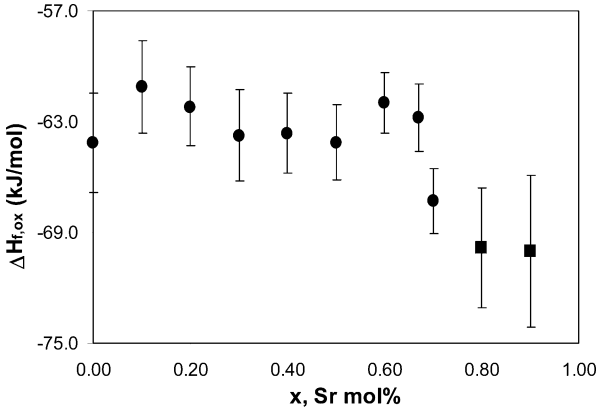

Figure 6. Enthalpies of formation from oxides for the $LaFeO_3$−$SrFeO_3$ solid solution system vs Sr content (x). The enthalpy data are from calorimetry (solid circle) or from extrapolation (solid square).

The enthalpy of formation data are practically independent of Sr composition at $x = 0-0.7$. Thus, the enthalpy of charge-coupled substitution involving oxidation in the solid solution, which is represented by eq 1, is close to zero. For samples with $x \geq 0.7$, the enthalpies of formation are about 5 kJ/mol more exothermic. However, considering the large uncertainties associated with them, the actual enthalpy difference between the samples with $x \geq 0.7$ and those with $x < 0.7$ may be smaller.

The energetic trend in Figure 6 can be explained in terms of the structures. For the two end-members, the structures are different, that is, orthorhombic for $LaFeO_3$[23] and cubic for $SrFeO_3$.[31] For intermediate compositions, structures from low symmetry (orthorhombic) to high symmetry (cubic) are expected; e.g., L40SF3.0 is determined as rhombohedral in this study. Our results generally agree with Dann et al.[28] who observed three crystallographically different regions in the $La_{1-x}Sr_xFeO_3$ system: orthorhombic at $0 \leq x \leq 0.2$, rhombohedral at $0.4 \leq x \leq 0.7$, and cubic at $0.8 \leq x \leq 1.0$. The enthalpy of formation from oxides appears to be slightly more exothermic in the composition range of $x \geq 0.7$ when the cubic structure is stable. Any difference in enthalpy between rhombohedral and orthorhombic structures cannot be resolved.

The enthalpies of formation for samples with $x \geq 0.7$ which were synthesized in air, i.e., L70SF2.97, L80SF2.96, and L90SF2.90, are more endothermic than those for fully oxidized counterparts. However, the latter, L70SF3.0, L80SF3.0, and L90SF3.0, are presumably not the most stable in air in terms of free energy. Instead, the stable compounds are partly reduced. A delicate balance between enthalpy and entropy of oxidation is sensitive to changes in oxygen partial pressure and temperature, resulting in a significant variation of oxygen nonstoichiometry with x, p_{O_2}, and T. In addition, creating oxygen vacancies in the structure may also be entropically favorable.

4. Conclusions

The $La_{1-x}Sr_xFeO_{3-\delta}$ solid solution system is a good example for studying the thermodynamic behavior of com-

(43) Bakken, E.; Allan, N. L.; Hugh, T.; Barron, K.; Mohn, C. E.; Todorov, I. T.; Stolen, S. *Phys. Chem. Chem. Phys.* **2003**, *5*, 2237.

plex oxides in a complete composition range where defect chemistry plays a major role. Oxygen nonstoichiometry (δ) is a function of the Sr doping amount, oxygen partial pressure, annealing temperature, and cooling rate. A large number of samples were prepared with varying synthesis conditions. Enthalpies of formation from oxides for all the samples were determined from high-temperature drop solution calorimetry and are interpreted in terms of redox between Fe^{3+} and Fe^{4+}, oxygen vacancy formation, vacancy short-range ordering, and structural phase transitions.

In each perovskite-type $La_{1-x}Sr_xFeO_{3-\delta}$ series with a given x, the enthalpies of formation is a linear function of oxygen deficiency. Thus, the enthalpies of formation for some perovskites samples which are not experimentally available, e.g., L80SF3.0, L90SF3.0, and L90SF2.55, can be extrapolated. This allows one to construct two complete solid solution systems, $LaFeO_3-SrFeO_{2.5}$ and $LaFeO_3-SrFeO_3$, in which all samples are perovskite-type.

In the maximally reduced solid solution, i.e., $LaFeO_3-SrFeO_{2.5}$, extensive short-range ordering of oxygen vacancies exists for $x > 0.5$, which is supported by three observations. First, the enthalpy of oxidation in each series is approximately a constant of -200 ± 50 kJ/mol O_2 for $0 < x \leq 0.5$ and -140 ± 30 kJ/mol O_2 for $0.5 < x < 1.0$. The more endothermic ΔH_{oxid} at $x > 0.5$ implies a stronger tendency of retaining oxygen vacancies, e.g., via short-range ordering. Second, as modeled by the two straight line segments in Figure 5b, when $x \leq 0.5$ (dilute range), the destabilization effect from oxygen vacancies is dominant and the enthalpy of vacancy formation is about 90 ± 11 kJ/mol $V_O^{\bullet\bullet}$. But when $x > 0.5$ (concentrated range), the system is stabilized by extensive short-range order. Third, extrapolation to the end-member ($x = 1$) in Figure 5 gives the enthalpy of formation of perovskite-type $SrFeO_{2.5}$ and the hypothetical brownmillerite−perovskite phase transition enthalpy at room temperature is estimated as 5.5 ± 4.0 kJ/mol. This small enthalpy corresponds to an entropy of transition significantly smaller than the configurational entropy assuming complete disorder after transition. The enthalpy of transition of L90SF2.55 from brownmillerite to perovskite is nearly zero at room temperature. These also suggest that extensive short-range order exists in the $La_{1-x}Sr_xFeO_{3-0.5x}$ samples with high x.

In the fully oxidized solid solution, i.e., $LaFeO_3-SrFeO_3$, the enthalpies of formation from oxides are virtually independent of Sr composition when $x < 0.7$ and are $\sim$5 kJ/mol more exothermic when $x \geq 0.7$. The overall trend is related to the structure evolution from orthorhombic ($0 \leq x \leq 0.2$) to rhombohedral ($0.4 \leq x \leq 0.7$) to cubic ($0.8 \leq x \leq 1.0$). Though the fully oxidized cubic samples have more exothermic enthalpy of formation, they are not the most stable phases in air in terms of free energy.

Acknowledgment. This project was supported by the U.S. Department of Energy (DOE) (Grant No. DEFG03-97ER45654).

CM048613O